

Supporting Information

In situ Coupling of CoP with MoO₂ for Enhanced Hydrogen Evolution

Jun Wang,^{a†} Hui Cheng,^{ab†} Shiyu Ren^a, Lili Zhang,^a Liang-Xin Ding,^{*a} and Haihui Wang^{*a}

a School of Chemistry and Chemical Engineering, South China University of Technology, Guangzhou, 510640, China

b Guangdong Institute of Analysis (China National Analytical Center, Guangzhou), Guangdong Academy of Sciences, Guangzhou, 510070, China

E-mail: lxding@scut.edu.cn, hhwang@scut.edu.cn

† J. Wang and H. Cheng contributed equally to this work.

S1. Experimental details

S1.1 Materials synthesis

Synthesis of porous CoP/MoO₂ thin films. All chemical reagents used in this study were analytical (AR) grade. Electrochemical deposition was carried out in a simple two-electrode electrolytic cell via galvanostatic electrodeposition, and the graphite electrode was used as a counter electrode (spectral grade). The details of the fabrication route are described in the following procedures: 1) Commercial carbon cloth (CC, AvCarb 1071 HCB, 1 cm × 1 cm) was employed as substrate. CoMoO₄ thin films were first electrodeposited from aqueous solutions of 0.02M Co(NO₃)₂, 0.02M Na₂MoO₄, and 0.05M NH₄NO₃ with current density of 0.6 mA cm⁻² for 30 min; 2) CoP/MoO_x-CC was obtained by heating CoMoO₄ thin films under the atmosphere of gaseous sodium hypophosphite at 300 °C in Ar flow for 2 hours; 3) Finally, porous CoP/MoO₂ thin films can be conveniently obtained by suspending CoP/MoO_x thin films in 1M KOH solution. Additionally, for comparison, the CoP thin films have also been prepared by the same route without Na₂MoO₄.

S1.2 Structural characterization

The morphologies and nanostructures of all the samples were characterized by scanning electron microscopy (SEM, FEI Nano430) and transmission electron microscope (TEM, JEOL 2100F). Raman spectra were collected using a Horiba Jobin Yvon LabRam Aramis Raman spectrometer equipped with a 632.8 nm laser. The composition and surface chemical state of the as-prepared samples were analyzed by X-ray photoelectron spectroscopy (XPS) using an ESCALAB 250 spectrometer (Thermo Fisher Scientific). All of the XPS spectra were corrected using C 1s peak at 284.8 eV.

SI.3 Electrochemical measurement

All of the electrochemical tests were carried out on a standard electrochemical workstation (IM6ex). Cyclic voltammetry (CV) and linear sweep voltammetry (LSV) measurements were conducted in 1M KOH solution with a typical three-electrode system. A Pt foil served as the counter electrode and a saturated calomel electrode (SCE) was used as the reference electrode. In this paper, all mentioned potentials were calibrated to versus the reversible hydrogen electrode (RHE), which is according to $E(RHE)=E(SCE)+0.2412+0.05916pH$.

Electrochemical capacitance is determined using CV measurements. The potential range is typically a 0.1 V window centered at open-circuit potential (OCP) of the system. CV measurements are conducted by sweeping the potential across the non-Faradaic region with different scan rates: from 2 mV/s to 10 mV/s. All measured current in this non-Faradaic potential region is assumed to be ascribed to the double-layer charging. The charging current, i_c , is then measured from CVs at multiple scan rates. The double-layer charging current is equal to the product of the scan rate, ν , and the electrochemical double-layer capacitance, C_{DL} , as given by eq (1).

$$i_c = \nu C_{DL} \quad (1)$$

Thus, a plot of i_c is acted as a function of ν yields a straight line with a slope equal to C_{DL} . The electrochemically active surface area (ECSA) of catalysts is calculated from the double-layer capacitance according to eq (2):

$$ECSA = C_{DL}/C_s \quad (2)$$

where C_s is the specific capacitance of catalyst or the capacitance of an atomically smooth planar surface of the material per unit area under identical electrolyte conditions. For our estimates of surface area, we use general specific capacitances of $C_s = 0.04 \text{ mF/cm}^2$ in 1M KOH.

SI.4 The first principles calculations

The first principles calculations in the framework of density functional theory, including structural, electronic performances, were carried out based on the Cambridge Sequential Total Energy Package known as CASTEP. The exchange–correlation functional under the generalized gradient approximation (GGA) with norm-conserving pseudopotentials and Perdew–Burke–Ernzerhof functional was adopted to describe the electron–electron interaction. An energy cutoff of 750 eV was used and a k-point sampling set of $5 \times 5 \times 1$ were tested to be converged. A force tolerance of 0.01 eV \AA^{-1} , energy tolerance of 5.0×10^{-7} eV per atom and maximum displacement of 5.0×10^{-4} \AA were considered. The model of amorphous CoP, CoMoO₄, MoO₂ and CoP/MoO₂ are built after relaxing the crystal surface at 2000K, and the ordered atomic arrangement has been damaged. The vacuum space along the z direction is set to be 15 \AA , which is enough to avoid interaction between the two neighboring images. All atoms were relaxed.

Adsorption energy ΔE of A group on the surface of substrates was defined as:

$$\Delta E = E_{*A} - (E_{*} + E_A)$$

where $*A$ and $*$ denote the adsorption of A group on substrates and the bare substrates, E_A denotes the energy of A group.

S2. Supplementary Figures and Tables

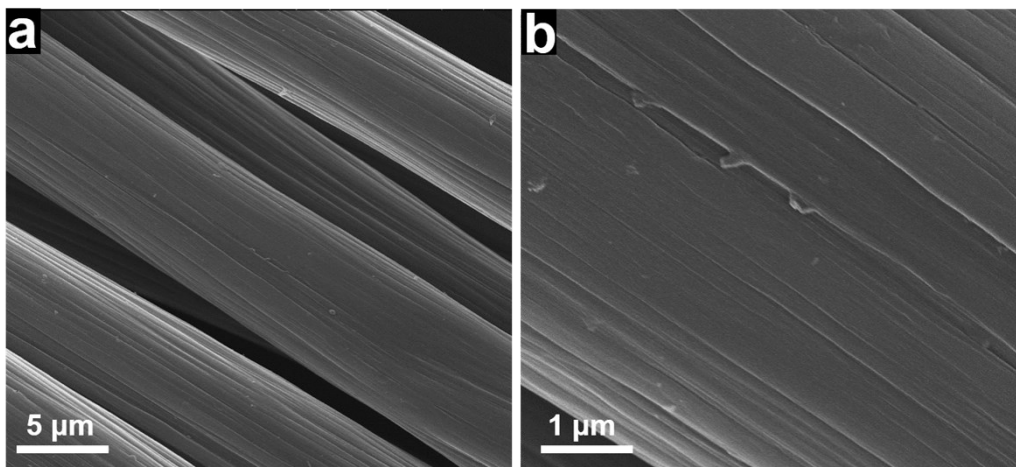


Figure S1. SEM images of the pure carbon cloth.

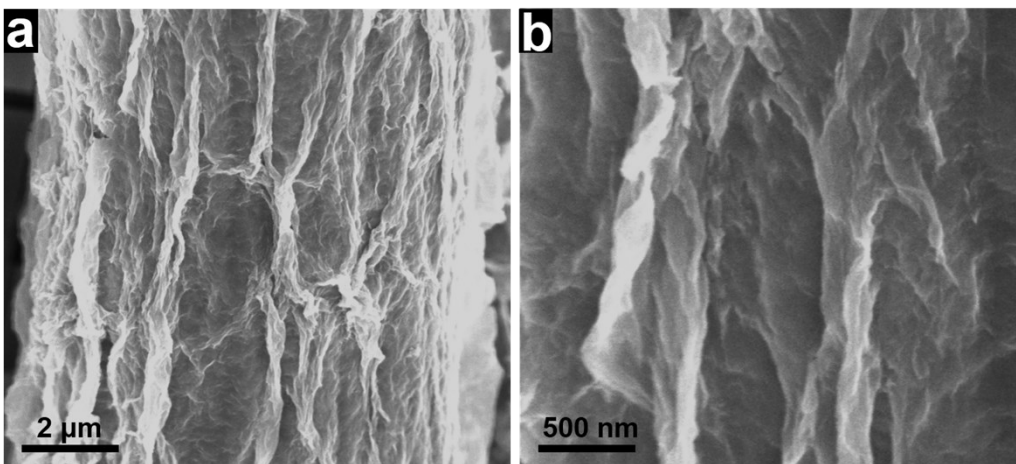


Figure S2. SEM images of the CoMoO₄ thin films.

Figure S2 reveals that the CoMoO₄ has been successfully deposited on the carbon cloth substrate and shows a thin films structure characteristic.

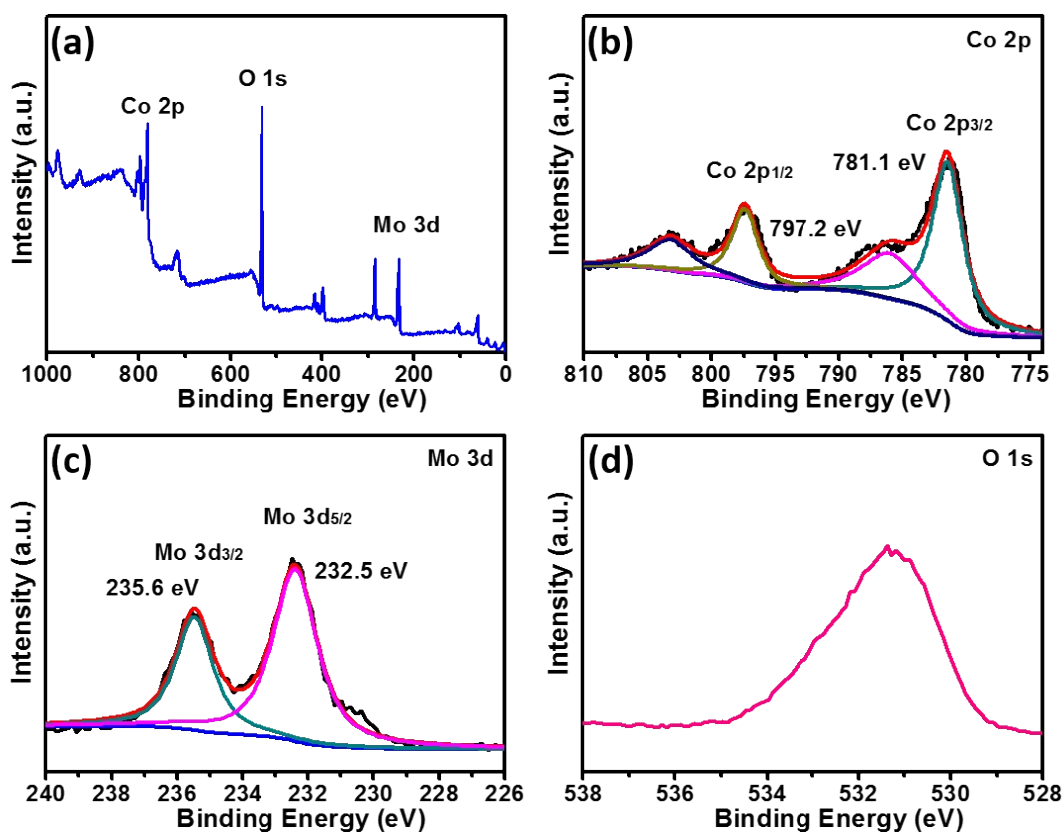


Figure S3. XPS spectra of the CoMoO₄: (a) survey, (b) Co 2p, (c) Mo 3d, and (d) O 1s spectra.

Figure S3 presents the XPS spectra of the CoMoO₄ sample. The survey spectrum shows that only Co, Mo, O are contained (Figure S3a). The Co 2p can be deconvoluted into two peaks (Figure S3b), located at 781.1 eV and 797.2 eV, which are consistent with Co²⁺ in CoMoO₄ phase.^[1-2] The spectrum of Mo 3d core level carries two peaks at 232.5 eV and 235.6 eV (Figure S3c), corresponding to Mo 3d_{5/2} and Mo 3d_{3/2}. The value of binding energy and the spacing of two peaks well coincide with the previous reported Mo⁶⁺.^[3] From the Figure S3d, only one typical peak (531.4 eV) is observed in O 1s spectrum, which is consistent with the binding energy of O 1s in CoMoO₄. So, we can infer that this intermediate product is CoMoO₄.

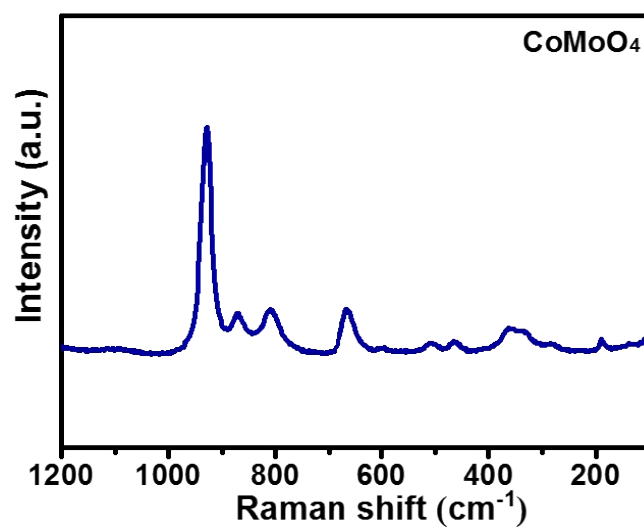


Figure S4. Raman spectrum of the CoMoO₄.

Raman spectrum was also carried out to have a further illustration of CoMoO₄. Figure S4 shows the Raman spectrum of CoMoO₄, with the intense band at 925 cm⁻¹ and some medium intensity bands at 869, 810, 658 and 351 cm⁻¹. Above mentioned bands are regarded as the characteristic peaks for CoMoO₄.^[4]

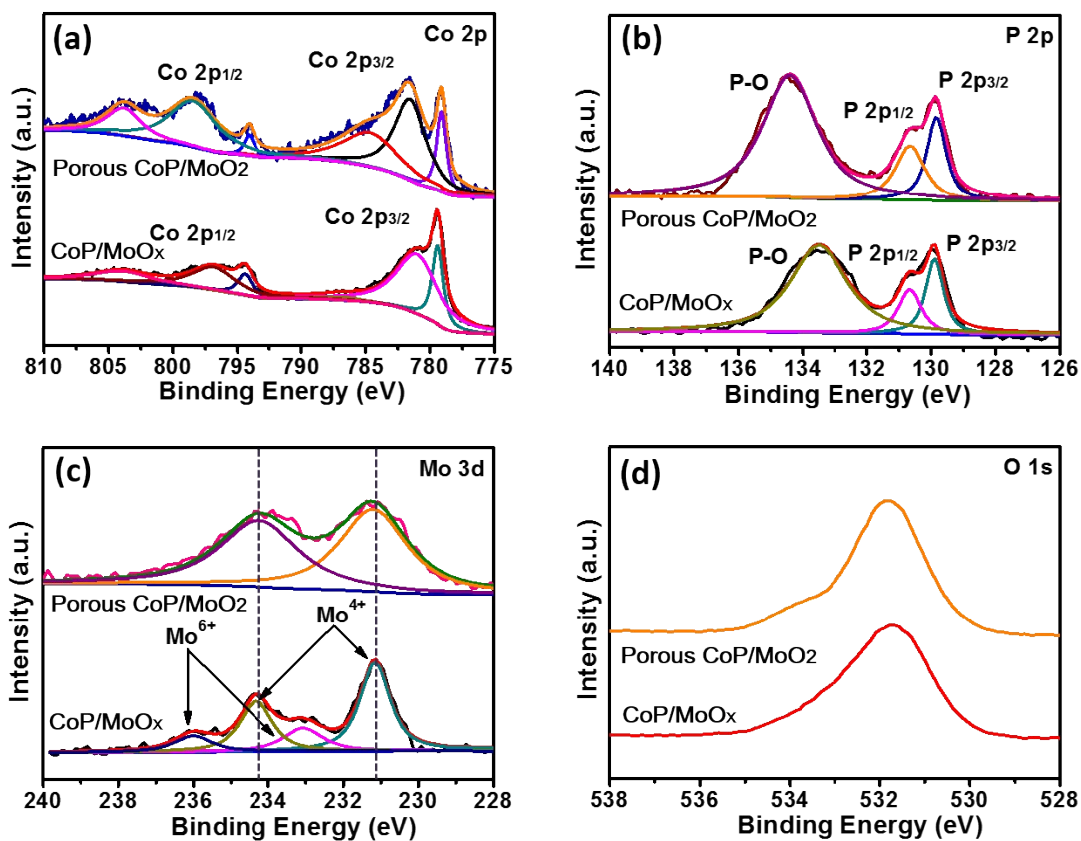


Figure S5. XPS spectra of CoP/MoO_x thin films and CoP/MoO₂ thin films: (a) Co 2p, (b) P 2p, (c) Mo 3d, and (d) O 1s spectra.

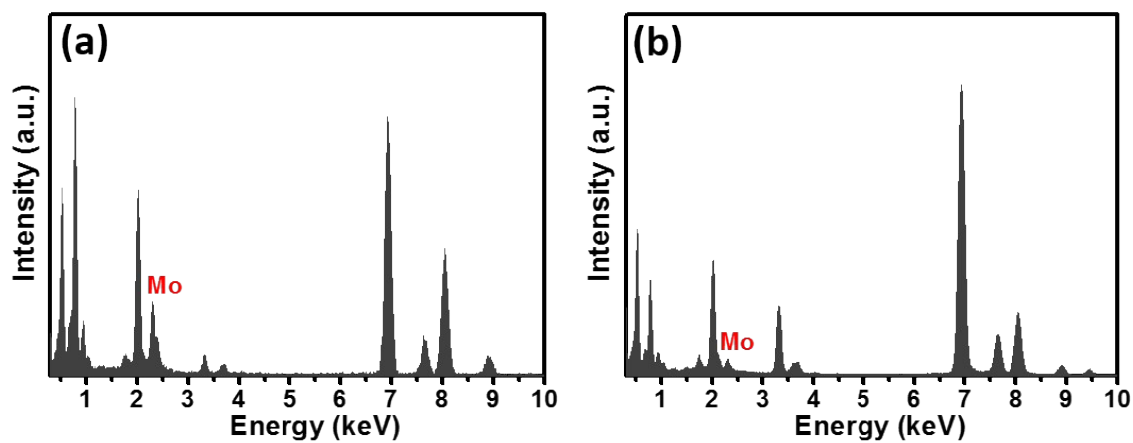


Figure S6. EDX patterns of (a) CoP/MoO_x thin films, and (b) CoP/MoO₂ thin films.

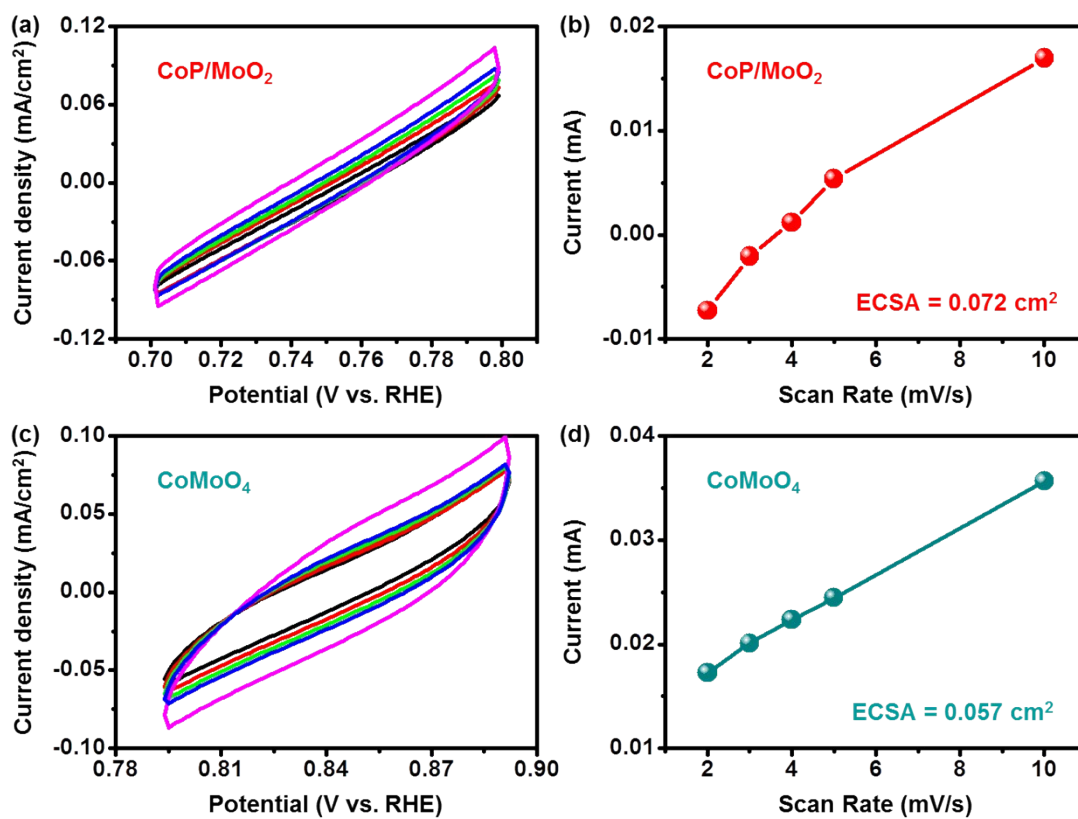


Figure S7. (a, c) Electrochemical capacitance of CoP/MoO₂ and CoMoO₄. (b, d) Charging current density plots with different scan rates (2, 3, 4, 5, 10 mV/s) for CoP/MoO₂ and CoMoO₄.

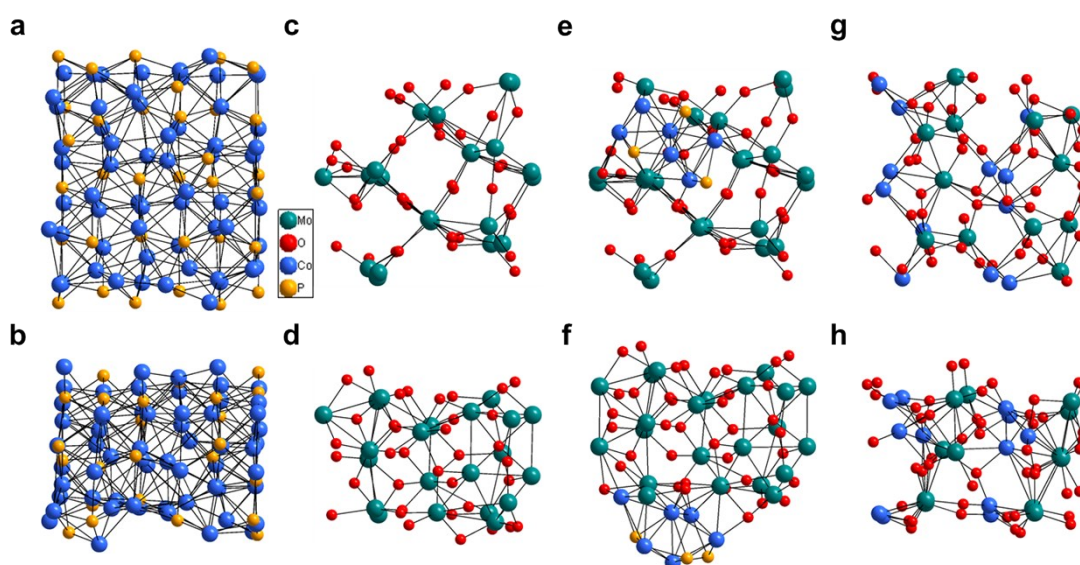


Figure S8. Simplified CoP (a-b), MoO₂ (c-d), CoP/MoO₂ (e-f) and CoMoO₄ clusters (g-h) for DFT calculations (a, c, e, g: Top view, b, f, d, h: Side view).

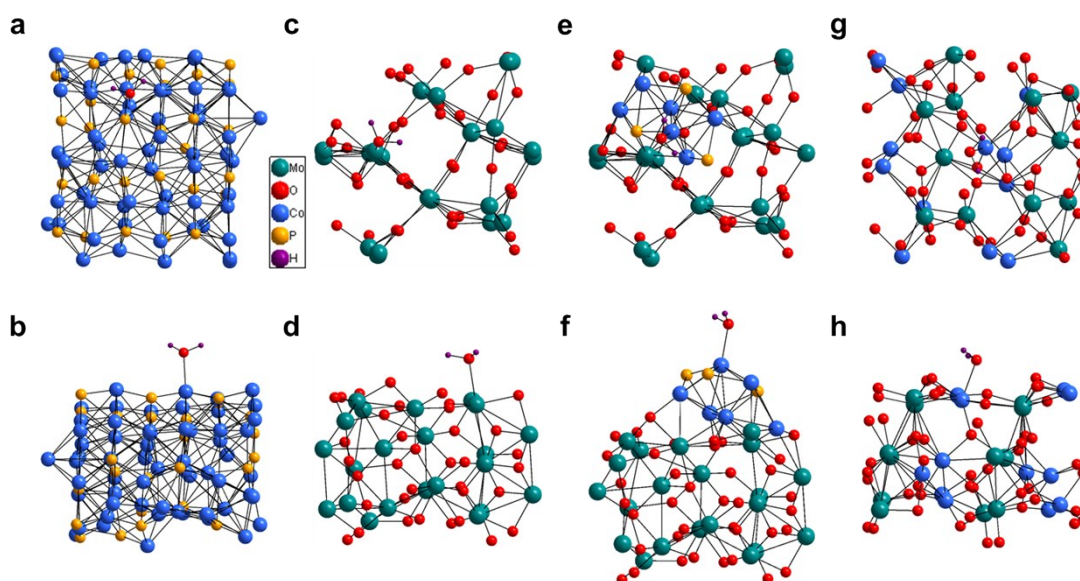


Figure S9. Simplified CoP (a-b), MoO₂ (c-d), CoP/MoO₂ (e-f) and CoMoO₄ clusters (g-h) with H₂O adsorption for DFT calculations (a, c, e, g: Top view, b, f, d, h: Side view).

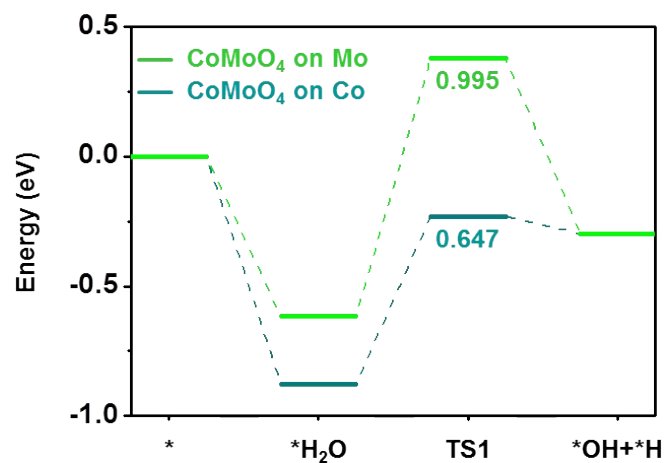


Figure S10. Calculated transition state adsorption energy diagram of HER for CoMoO₄ on Co and Mo, in which TS1 represent the energy barrier for the reaction.

Figure S10 shows the Volmer catalytic process of H₂O at the Co and Mo active sites in CoMoO₄. By comparison, the adsorption energy of H₂O at the active site of Co is larger and the energy barrier to be overcome in the decomposition process is smaller. Therefore, it is consider that Co rather than Mo is the active site for CoMoO₄.

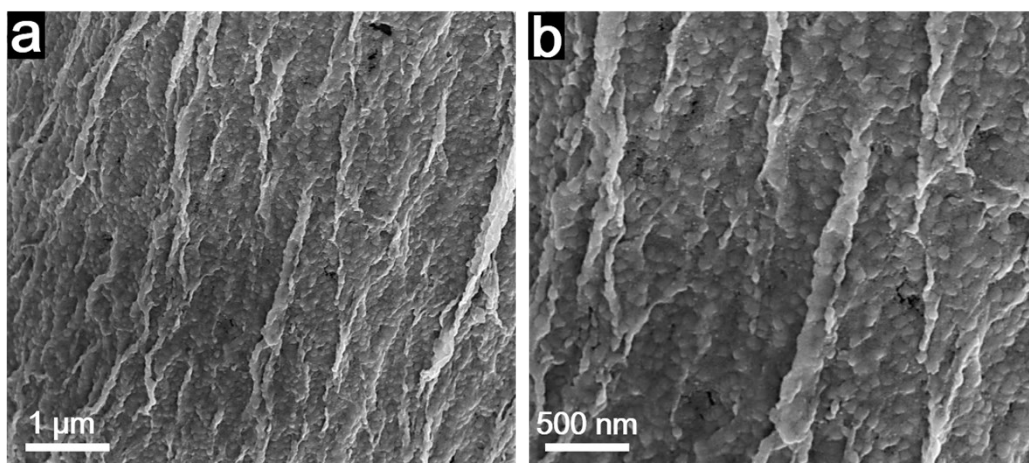


Figure S11. SEM images of the imporous CoP/MoO₂ thin films (prepared by repeated phosphatizing).

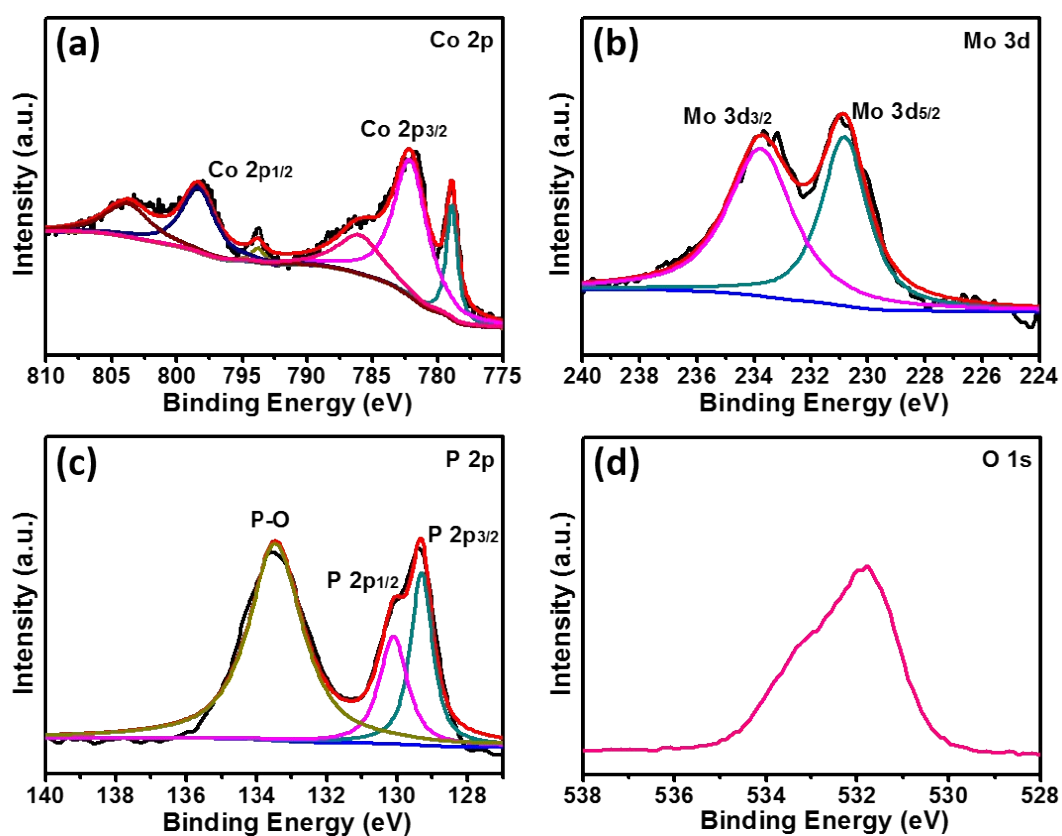


Figure S12. XPS spectra of the imporous CoP/MoO₂ thin films: (a) Co 2p, (b) Mo 3d, (c) P 2p, and (d) O 1s spectra.

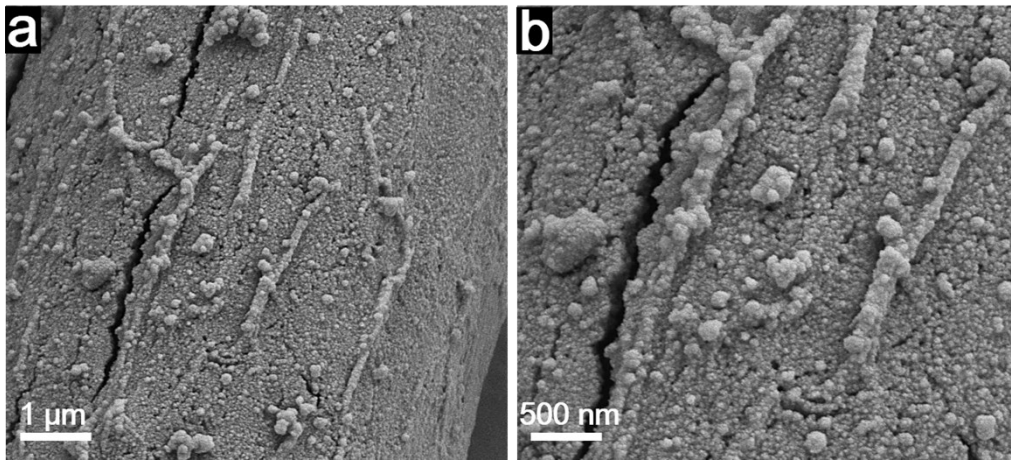


Figure S13. SEM images of the porous CoP/MoO₂ thin films after accelerated durability test.

Table S1. Comparison of HER performance of porous CoP/MoO₂ with some previous-reported non-precious metal HER electrocatalysts.

Author	Catalyst	Onset overpotential	Overpotential at 10 or 20 mA cm ⁻²
This work	Porous CoP/MoO₂	12mV	29 mV (10 mA cm⁻²) 41 mV (20 mA cm⁻²)
Adv. Mater. 2015,10,1002	Co(OH) ₂ @PANI	50 mV	90 mV (10 mA cm ⁻²)
Angew. Chem. Int. Ed. 2014, 53, 9577	Cu ₃ P	62 mV	143 mV (10 mA cm ⁻²)
ACS Sustainable Chem. Eng. 2019, 7, 12501-12509	CoNiS _x /CFP		123 mV (10 mA cm ⁻²)
Nanoscale, 2018,10, 2603-2612	CoP@NPMG	125 mV	91 mV (10 mA cm ⁻²)
Angew. Chem. Int. Ed. 2014, 53, 12594	CoS ₂ /RGO		142 mV (10 mA cm ⁻²)
Nano Lett. 2015, 15, 6015–6021	Co/Co ₃ O ₄	30 mV	90 mV (10 mA cm ⁻²)
Angew. Chem. Int. Ed. 2015, 54, 10752	Mo ₂ C@NC	60 mV	124 mV (10 mA cm ⁻²)
ACS Energy Letters. 2019, 4, 12, 2830-2835	MoS ₂		153 mV (10 mA cm ⁻²)
Mater. Chem. Front., 2019,3, 1872-1881	MoP@NPCF/C C		115 mV (10 mA cm ⁻²)
Angew. Chem. Int. Ed. 2020, 59, 3544-3548	Mo ₂ C-MoO _x /CC	28 mV	60 mV (10 mA cm ⁻²)
Small 2017, 1602866	MoSe ₂	91 mV	

References:

- [1] J. Yao, Y. Gong, S. Yang, P. Xiao, Y. Zhang, K. Keyshar, G. Ye, S. Ozden, R. Vajtai, P. M. Ajayan, *ACS Appl. Mater. Inter.* **2014**, *6*, 20414-20422.
- [2] M. Q. Yu, L. X. Jiang, H. G. Yang, *Chem. Commun.* **2015**, *51*, 14361-14364.
- [3] X. Xia, W. Lei, Q. Hao, W. Wang, X. Wang, *Electrochem. Acta* **2013**, *99*, 253-261.
- [4] X. Xu, J. Shen, N. Li, M. Ye, *J. Alloy Compd.* **2014**, *616*, 58-65.